Volume 14 - Issue 6 (2025)

Journal of Transportation Science and Technology

Journal homepage: https://tapchicongnghegtvt.vn

Dual Laser-Aided UAV Motion Compensation for Vision-Based Displacement Measurement of High-Speed Railway Bridge

Truong Thanh Chung [1,2,*], Tran Quang Huy[1], Dang Quoc My[1], Tran Ngoc Hoa[2], Bui Tien Thanh[2], Guido De Roeck[3]

[1]*Nha Trang University, Vietnam*
[2]*University of Transport and Communications, Vietnam*
[3]*KU Leuven, Belgium*

Keywords:

Unmanned Aerial Vehicles (UAV)

Computer vision

Camera vibration compensation

High-speed railway bridge

ABSTRACT

Unmanned Aerial Vehicles (UAVs) offer mobility and flexibility for vision-based structural health monitoring but are susceptible to motion-induced errors in displacement tracking. This study proposes a dual-laser compensation method in which two fixed laser beams, projected near the target to serve as reference points, are tracked to estimate UAV translation and rotation via affine transformation. By removing this motion component from the measured signal, the actual structural displacement can be obtained. Validation through both laboratory and field tests on a railway bridge demonstrates the effectiveness of the proposed method.

1. Introduction

Unmanned Aerial Vehicles (UAVs) have emerged as effective tools for structural health monitoring (SHM), offering rapid deployment, large-area coverage, and vision-based non-contact displacement monitoring [1]. However, UAV mobility introduces motion errors caused by wind, control inaccuracies, and navigation noise, which complicate the separation of true structural motion from camera movement [2].

Existing correction approaches include applying high-pass filtering to vibration data [3], using pixels assumed to be stationary within the frame [4], and employing sensors to measure camera vibrations [5]. However, these methods have inherent limitations; for example, stationary pixels may not exist in certain scenarios, such as in mid-span frames of a bridge [6], and additional onboard sensors increase system complexity and payload weight. Moreover, filtering techniques can inadvertently attenuate low-frequency structural responses that are critical for evaluating bridge behavior under operational loads.

In this study, we propose a novel dual-laser–aided vision correction method. Two fixed, ground-based laser points are projected onto the bridge, and their apparent motion in the UAV video is used to estimate

*Truong Thanh Chung, Nha Trang University, Vietnam.
Email: chungtt@ntu.edu.vn

https://www.doi.org/10.55228/JTST140406
Received: August 24, 2025; Received in revised: October 05, 2025; Accepted: October 31, 2025
Available online: November 15, 2025
pISSN: 1859-4263; eISSN: 3030-4261

an affine transformation representing UAV-induced movement. This approach enables simultaneous correction of both translational and rotational camera motions. By removing the motion component from the observed target displacement, the actual structural displacement can be obtained. The performance of the proposed method is validated through laboratory tests and field experiments on operational railway bridges, demonstrating its potential for accurate, non-contact displacement monitoring in challenging field conditions.

2. Theoretical background

2.1. Computer Vision-Based Displacement Measurement with Sub-Pixel Refinement

In this study, the template matching method [7] was used to track the target's movement in the video frames. Zero-mean normalized cross-correlation (ZNCC) was applied, as it is insensitive to offset and linear changes in illumination [8].

$$C_{\mathrm{ZNCC}} = \sum_{i=-M}^{M}\sum_{j=-N}^{N} \frac{\left(f\left(x_i, y_j\right) - f_m\right)\left(g\left(x'_i, y'_j\right) - g_m\right)}{\Delta f\ \Delta g} \quad (1)$$

Where $f\left(x_i, y_j\right)$ and $g\left(x'_i, y'_j\right)$ represent the image intensity values in the template region and the new frame, respectively; f_m and g_m are the average intensity values in the template region and the new frame; Δf and Δg denote the standard deviations of the intensity values in the template region and the new frame.

The integer-pixel location obtained from the ZNCC matrix provides only a coarse estimate of the target displacement. To further improve displacement measurement accuracy, sub-pixel tracking using the quadratic interpolation method [9] was implemented. The normalized cross-correlation matrix around the best match is locally approximated using a second-order (quadratic) surface:

$$S\left(x, y\right) = ax^2 + bxy + cy^2 + dx + ey + f \quad (2)$$

To fit this surface, a 3×3 neighborhood around the maximum point $\left(x_i, y_j\right)$ in the similarity matrix is selected, yielding 9 known similarity values. Then the subpixel maximum $\left(x_s, y_s\right)$ of the surface is found by setting the gradients to zero:

$$\frac{\partial S}{\partial x} = 2ax + by + d = 0 \quad (3)$$

$$\frac{\partial S}{\partial y} = 2cy + bx + e = 0 \quad (4)$$

Solving this linear system yields the refined displacement in sub-pixel units relative to the integer peak location.

$$x_s = \frac{2ce - bd}{b^2 - 4ac} \quad (5)$$

$$y_s = \frac{2ad - be}{b^2 - 4ac} \quad (6)$$

The total displacement is the integer-pixel estimate plus the sub-pixel correction in Equations (5)-(6). An illustration of the sub-pixel refinement using quadratic interpolation is shown in Figure 1. Figure 1a presents the coarse ZNCC values on a 3×3 pixel grid, and Figure 1b shows the quadratic surface fitted to this 3×3 neighborhood. The new extremum, marked by a triangle, indicates the refined sub-pixel best-matching location.

a) **b)**

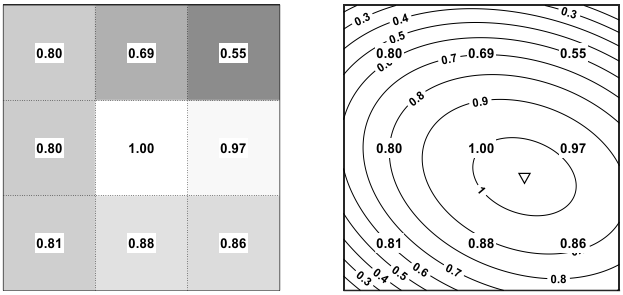

Figure 1. Quadratic peak refinement. (a) 3×3 correlation values, (b) fitted quadratic surface.

2.2. Dual-Laser Correction Using Affine Transformation

During measurement, the UAV experienced significant motions, including both translation and rotation, as shown in Figure 2. In earlier research [10], a single laser beam was projected from a fixed ground location onto the structure, and the apparent motion of the laser spot was subtracted from the measured target displacement to estimate the true structural displacement.

$$D_{\mathrm{true}} = D_{\mathrm{measured}} - D_{\mathrm{laser}} \quad (7)$$

Where D_{true} denotes the true displacement of the target, D_{measured} is the apparent displacement of the target measured from the UAV video, and D_{laser} is the apparent motion of the laser spot.

The single-laser approach assumes that the laser spot experiences the same apparent motion as the target—an assumption valid only under ideal conditions when the laser spot is vertically aligned beneath the target in the camera frame (Figure 3a). In practice, the laser may be projected from hundreds of meters away, making perfect vertical alignment impractical. When the laser and target are laterally separated, UAV rotation induces different apparent motions for each, violating the equal-motion assumption and reducing compensation accuracy.

To address these limitations, we propose a dual-laser vision-based correction method (Figure 3b). Two laser beams are projected from the ground onto stable reference points near the measurement target. Tracking the apparent motion of both laser spots in the UAV's camera frame enables estimation of the UAV's rigid-body motion parameters—translation and rotation.

Let the coordinates in the initial frame as follows. The laser 1 and laser 2 has the coordinate of (x_{L1}, y_{L1}) and (x_{L2}, y_{L2}); the coordinate of the target is (x_T, y_T). In the next frame, the laser 1 and laser 2 has the coordinate of (x'_{L1}, y'_{L1}) and (x'_{L2}, y'_{L2}); the coordinate of the target is (x_T', y_T').

The rotation angle of the frame is calculated as

$$\theta = \operatorname{atan}\left(y_{L2} - y_{L1},\, x_{L2} - x_{L1}\right) - \operatorname{atan}\left(y'_{L2} - y'_{L1},\, x'_{L2} - x'_{L1}\right) \tag{8}$$

The translation vector of the frame is calculated as

$$\begin{bmatrix} t_x \\ t_y \end{bmatrix} = \begin{bmatrix} x_{L1} \\ y_{L1} \end{bmatrix} - \mathbf{R} \begin{bmatrix} x'_{L1} \\ y'_{L1} \end{bmatrix} \tag{9}$$

where **R** is rotation matrix

$$\mathbf{R} = \begin{bmatrix} \cos\theta & -\sin\theta \\ \sin\theta & \cos\theta \end{bmatrix} \tag{10}$$

The apparent target displacement due to UAV movement is

$$\begin{bmatrix} \hat{x}_T \\ \hat{y}_T \end{bmatrix} = \mathbf{R} \begin{bmatrix} x'_T \\ y'_T \end{bmatrix} + \begin{bmatrix} t_x \\ t_y \end{bmatrix} \tag{11}$$

The true vertical displacement of the target is

$$D_{true} = y'_T - \hat{y}_T \tag{12}$$

It is noted that when UAV rotation θ = 0, the rotation matrix R becomes the identity matrix. Therefore, Equation (12) simplifies to Equation (7), as only translational motion remains.

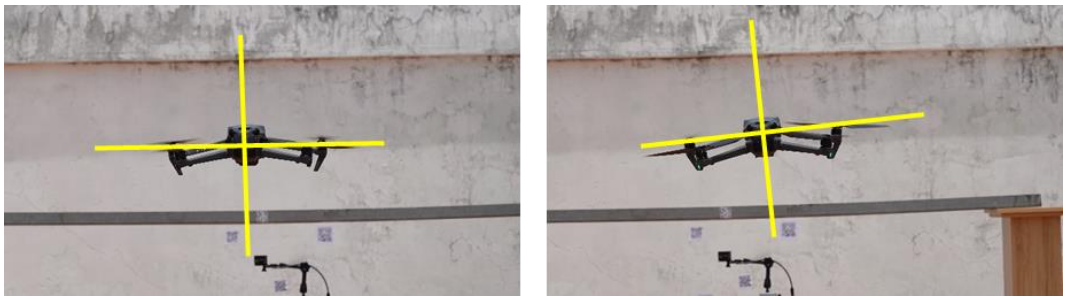

Figure 2. UAV translation and rotation during displacement measurement.

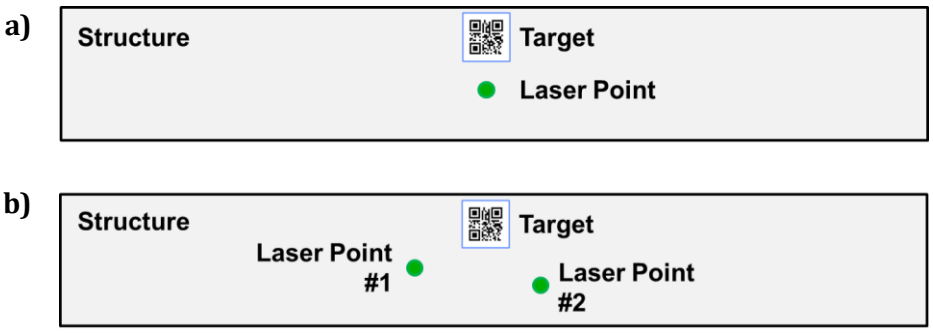

Figure 3. UAV movement compensation using. (a) Single laser point, (b) dual laser points.

2. Experiments and Results

2.1. Laboratory experiments

The laboratory experiment setup is shown in Figure 4. A UAV (DJI Mavic 3 Pro) was used to measure the displacement of a laboratory-scale steel beam. The total length of the beam is 2 meters and simply supported at both ends. To induce displacement, a person walked from one end of the beam to the other three times during the measurement period. The video was recorded at a frame rate of 120 fps with a resolution of 4096 × 2160 pixels. During measurement, the UAV hovered at a distance of approximately 5 meters from the beam.

Two green laser pointers (500 mW, 532 nm) were positioned approximately 12 m from the beam, each mounted on a rigid, heavy tripod to ensure stability and eliminate vibration during measurements. A high-precision displacement sensor (Micro-Epsilon ILD 1420-500, 2 kHz sampling rate) was installed beneath the beam, projecting its laser beam perpendicularly onto the steel surface. This sensor provided reference measurements of the beam's true displacement at the target point.

The displacement results are shown in Figure 5. Figure 5a presents the apparent displacement of the target and laser points, representing the displacement measured by the UAV without any compensation for UAV motion. As observed, the displacement fluctuates significantly, with a peak-to-peak value of approximately 120 mm. After compensation, the displacement of the target closely matches the true displacement measured by the laser sensor (Figure 5b).

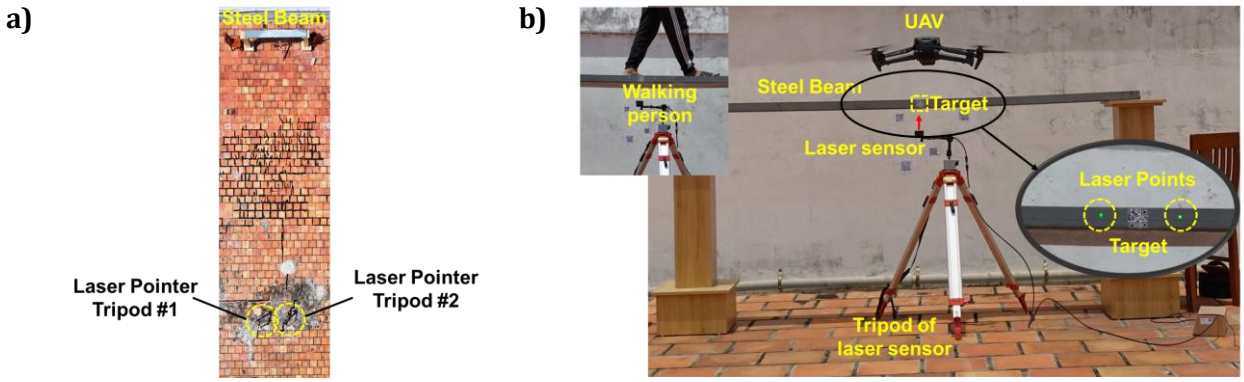

Figure 4. Experimental setup of laboratory experiments.

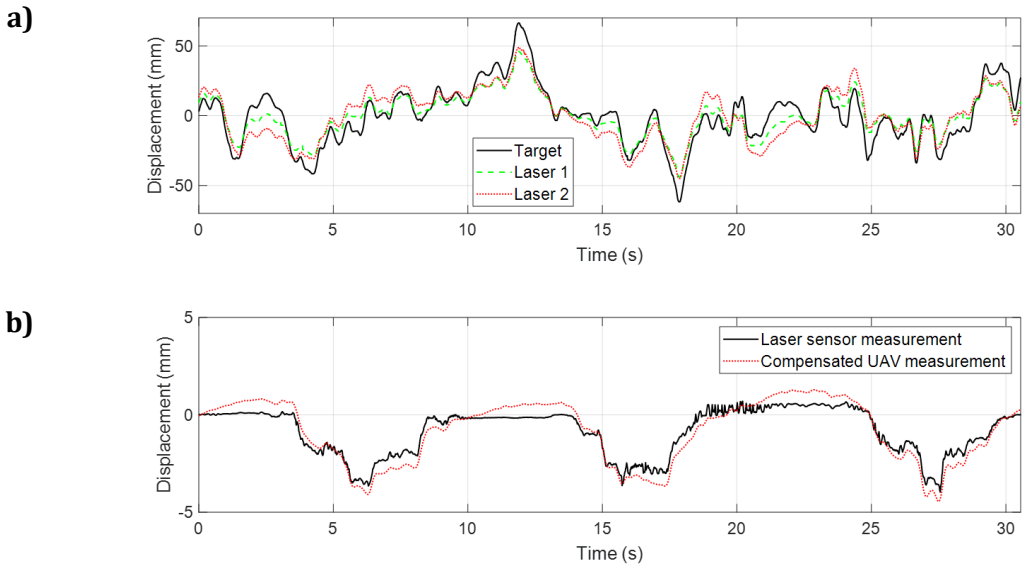

Figure 5. Comparison of laser-measured and UAV-measured displacements before and after motion compensation. (a) Apparent displacement of the target and laser points, (b) Displacement measured by laser sensors compared with compensated UAV measurement.

2.2. Tắc River Bridge Field Test

As shown in Figure 6, the field test was conducted on a railway truss bridge crossing the Tắc River, with a total span length of 66.3 m and a design load of 14 tons. Two laser pointers were mounted on separate tripods positioned approximately 120 m from the target. For displacement reference, a Sony RX100 VII camera was mounted on a tripod at the same location as the laser pointers, recording at a frame rate of 30 fps and a resolution of 3840 × 2160 pixels. The measurement was carried out on a sunny day with moderate wind conditions.

To synchronize the UAV and the Sony camera, one of the laser pointers was switched on and off at the beginning of the recording. The two video streams were then aligned in post-processing by matching the frames in which the laser changed from the off state to the on state.

A steel plate with a printed QR code measuring 200 × 200 mm was installed on the bridge. Using a QR code as the target offers two main advantages. First, it ensures that the target can be automatically and reliably detected without the need for manual selection of the target area—a process that can introduce errors. For example, if during target selection pixels belonging to a different structure or the background are mistakenly included, the measurement will be incorrect. Second, the scaling factor for converting between world coordinates and pixel coordinates can be automatically calculated using the known dimensions of the QR code.

Figure 7a shows the displacement of the target obtained from UAV video data before applying dual-laser motion compensation. The apparent displacement of the target and laser points is large due to UAV movement, with a peak-to-peak amplitude of approximately 300 mm. After applying the dual-laser compensation, the displacement becomes much smaller and closely matches the actual movement of the bridge. The results from the fixed camera are similar to those from the UAV, but appear smoother because the Sony camera's frame rate is much lower than that of the UAV (Figure 7b).

We compared the compensated UAV-derived displacement of the target with the reference displacement measured by the fixed Sony camera. Agreement was evaluated using the root-mean-square error (RMSE), mean absolute error (MAE), and Pearson correlation coefficient (r). The compensated UAV signal closely tracked the reference, showing RMSE of 4.35 mm, MAE of 3.37 mm, and a high correlation (r = 0.91). However, occasional peaks discrepancies remained quite large (≈ 20 mm), primarily due to two factors as follows.

First, the fixed camera used as the reference was positioned at a long stand-off distance from the structure and was not actively stabilized. Because the projected laser spots on the structure were too small to be visible from that distance, the fixed camera could not apply the same dual-laser compensation as the UAV. Consequently, its measurements were affected by tripod vibrations and wind-induced sway. Given the long focal length and large pixel-to-millimeter scale factor, even sub-pixel image jitter could result in several millimeters of apparent displacement. Thus, part of the reported discrepancy (RMSE = 4.35 mm, occasional peaks ≈ 20 mm) likely originated from motion of the unstabilized reference camera, rather than inaccuracy of the UAV-based measurement.

Second, minor out-of-plane (z-axis) UAV motion may have induced small apparent scale and perspective variations that cannot be fully modeled by the two-point affine compensation. These transient effects occasionally caused short spikes in the displacement difference but did not alter the overall displacement trend.

Table 1. Error metrics comparing compensated UAV displacement with the reference.

RMSE (mm)	MAE (mm)	Pearson correlation
4.35	3.37	0.91

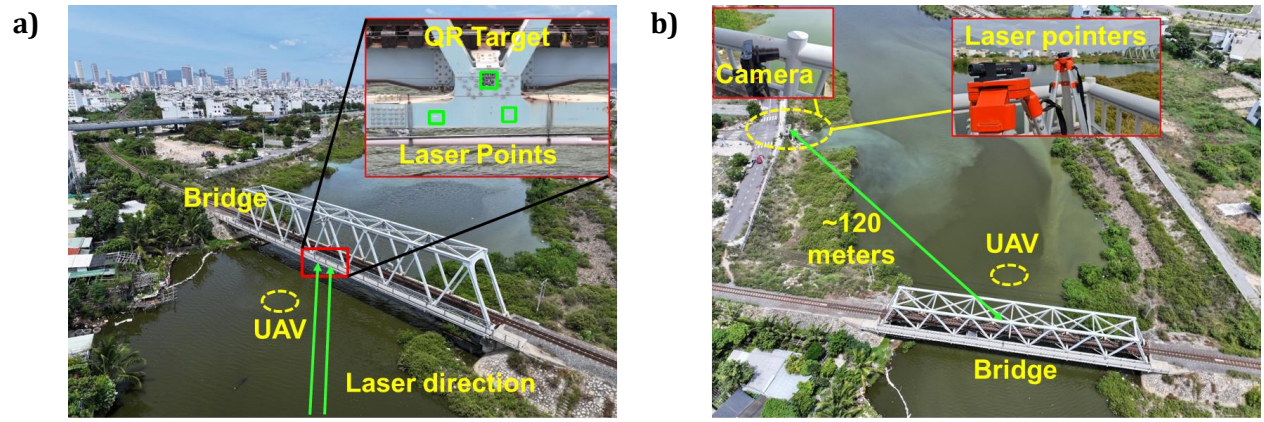

Figure 6. Tắc River Bridge Field Test (June 25, 2025). (a) UAV setup and laser points projected onto the QR target on the bridge beam, (b). Location of the fixed camera and laser assembly positioned away from the bridge.

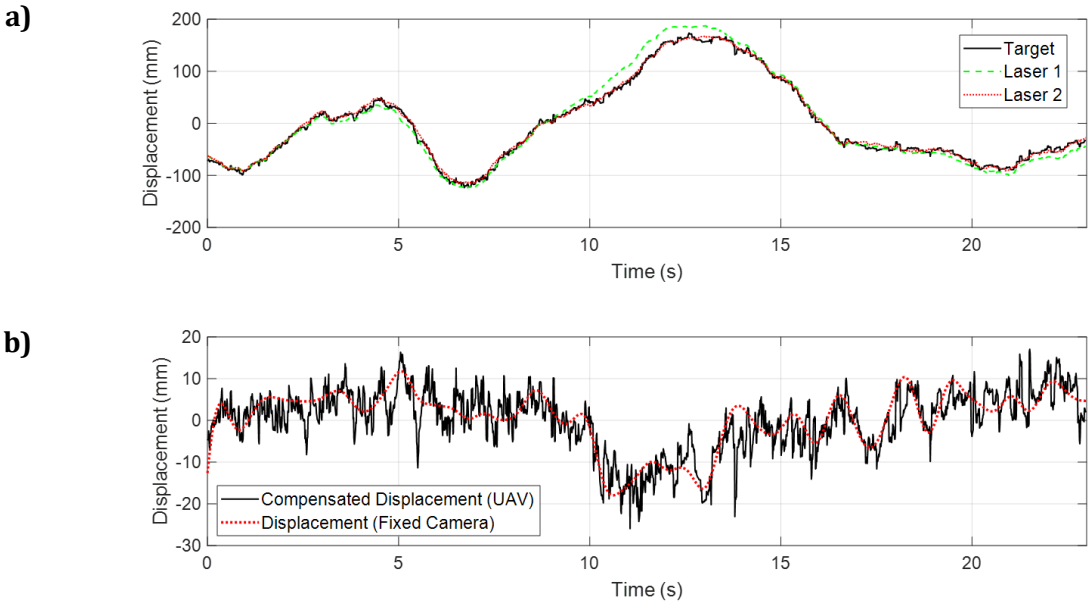

Figure 7. Comparison of laser-measured and UAV-measured displacements before and after motion compensation. (a) Apparent displacement of the target and laser points, (b) Displacement measured by fixed camera (Sony RX100 VII) compared with compensated UAV measurement.

3. Conclusion

This study proposed and validated a dual-laser motion compensation method for UAV-based vision displacement measurement of railway bridges. By projecting two fixed laser beams onto reference points near the measurement target, UAV-induced translation and rotation were estimated through affine transformation and subsequently removed from the measured signal, allowing accurate recovery of the true structural displacement. The method was verified through both laboratory and field tests on an operational railway bridge, demonstrating a significant improvement in measurement accuracy compared with uncompensated UAV data. These findings highlight the potential of the proposed dual-laser approach for enhancing non-contact, vision-based displacement monitoring in dynamic bridge environments.

In future work, the reference camera will be actively stabilized using in-frame fiducial markers or laser references to ensure a more reliable ground truth. Moreover, the UAV compensation framework will be extended to employ three non-collinear reference points to estimate a full planar homography, thereby improving robustness against perspective and scale variations.

Contributions of authors in this article

Truong Thanh Chung: Methodology, Data Collection, Investigation, Validation, Writing–

original manuscript, Feedback on peer review. **Tran Quang Huy:** Data Collection. **Dang Quoc My:** Data Collection. **Tran Ngoc Hoa:** Methodology, Supervision, Manuscript Editing. **Bui Tien Thanh:** Methodology, Supervision, Manuscript Editing. **Guido De Roeck:** Methodology, Supervision.

Acknowledgments

This research is funded by Nha Trang University for science and technology under grant number TR2024-13-25.

Declaration of competing interest and dedication to copyright

We have no conflicts of interest to disclose and confirm that this work has not been previously published.

Data available

Data will provided upon request.

1st Truong Thanh Chung*. *Nha Trang University, Vietnam*

2nd Tran Quang Huy. *Nha Trang University, Vietnam*

3rd Dang Quoc My. *Nha Trang University, Vietnam*

4th Tran Ngoc Hoa. *University of Transport and Communications, Vietnam*

5th Bui Tien Thanh. *University of Transport and Communications, Vietnam*

6th Guido De Roeck. *KU Leuven, Belgium*

*Corresponding author: chungtt@ntu.edu.vn

References

[1] X. W. Ye, C. Dong, T. Liu, and D. Dai, "Vision-based structural displacement measurement: Current status and future trends," *Engineering Structures*, vol. 210, Art. no. 110416, 2020, doi: 10.1016/j.engstruct.2020.110416.

[2] H. Lee, J. W. Park, and Y. Kim, "UAV-based displacement measurement with motion compensation using reference markers," *Sensors*, vol. 22, no. 5, Art. no. 1852, 2022, doi: 10.3390/s22051852.

[3] V. Hoskere, et al., "Vision-based modal survey of civil infrastructure using unmanned aerial vehicles," *Journal of Structural Engineering*, vol. 145, no. 7, Art. no. 04019062, 2019, doi: 10.1061/(ASCE)ST.1943-541X.0002329.

[4] Y. Han, G. Wu, and D. Feng, "Vision-based displacement measurement using an unmanned aerial vehicle," *Structural Control and Health Monitoring*, vol. 29, no. 10, Art. no. e3025, 2022, doi: 10.1002/stc.3025.

[5] D. Ribeiro, et al., "Non-contact structural displacement measurement using unmanned aerial vehicles and video-based systems," *Mechanical Systems and Signal Processing,* vol. 160, Art. no. 107869, 2021, doi: 10.1016/j.ymssp.2021.107869.

[6] H. Habeenzu, et al., "UAS-based bridge displacement measurement using two cameras with non-overlapping fields of view," *Automation in Construction*, vol. 167, Art. no. 105687, 2024, doi: 10.1016/j.autcon.2024.105687.

[7] Y. Xu and J. M. W. Brownjohn, "Review of machine-vision based methodologies for displacement measurement in civil structures," *Journal of Civil Structural Health Monitoring*, vol. 8, pp. 91–110, 2018, doi: 10.1007/s13349-017-0261-4.

[8] R. Szeliski, *Computer Vision: Algorithms and Applications*, 2nd ed. City, Country: Springer, 2022.

[9] D. Zhang, et al., "A high-speed vision-based sensor for dynamic vibration analysis using fast motion extraction algorithms," *Sensors*, vol. 16, no. 4, Art. no. 572, 2016, doi: 10.3390/s16040572.

[10] C. Zhang, et al., "A two-stage correction method for UAV movement-induced errors in non-target computer vision-based displacement measurement," *Mechanical Systems and Signal Processing*, vol. 224, Art. no. 112131, 2025, doi: 10.1016/j.ymssp.2025.112131.